Linear distributed inverse solutions for interictal eeg source localisation

Carboni, Margherita; Brunet, Denis; Seeber, Martin; Michel, Christoph; Vulliemoz, Serge; Vorderwulbecke, Bernd

Clinical Neurophysiology 133 (2022) 58–67

Contents lists available at ScienceDirect

Clinical Neurophysiology

journal homepage: www.elsevier.com/locate/clinph

Linear distributed inverse solutions for interictal EEG source localisation

Margherita Carboni [a,b], Denis Brunet [b], Martin Seeber [b], Christoph M. Michel [b], Serge Vulliemoz [a], Bernd J. Vorderwülbecke [a,c,1,*]

[a] EEG and Epilepsy Unit, University Hospitals and Faculty of Medicine, University of Geneva, Rue Gabrielle-Perret-Gentil 4, 1205 Geneva, Switzerland
[b] Functional Brain Mapping Lab, Department of Basic Neurosciences, University of Geneva, Campus Biotech, 9 Chemin des Mines, 1202 Geneva, Switzerland
[c] Epilepsy-Center Berlin-Brandenburg, Department of Neurology, Charité – Universitätsmedizin Berlin, Charitéplatz 1, 10117 Berlin, Germany

ARTICLE INFO

Article history:
Accepted 9 October 2021
Available online 08 November 2021

Keywords:
Minimum Norm
Weighted Minimum Norm
LORETA
Local Autoregressive Average
sLORETA
eLORETA

HIGHLIGHTS

- Spatial accuracy of 6 linear distributed inverse solutions for interictal high-density EEG source localisation was evaluated.
- Low-Resolution Electromagnetic Tomography and Local Autoregressive Average best localised both patients' and simulated sources.
- These two algorithms' superiority over newer inverse solutions was due to their relative robustness towards noise.

ABSTRACT

Objective: To compare the spatial accuracy of 6 linear distributed inverse solutions for EEG source localisation of interictal epileptic discharges: Minimum Norm, Weighted Minimum Norm, Low-Resolution Electromagnetic Tomography (LORETA), Local Autoregressive Average (LAURA), Standardised LORETA, and Exact LORETA.
Methods: Spatial accuracy was assessed clinically by retrospectively comparing the maximum source of averaged interictal discharges to the resected brain area in 30 patients with successful epilepsy surgery, based on 204-channel EEG. Additionally, localisation errors of the inverse solutions were assessed in computer simulations, with different levels of noise added to the signal in both sensor space and source space.
Results: In the clinical evaluations, the source maximum was located inside the resected brain area in 50–57% of patients when using LORETA or LAURA, while all other inverse solutions performed significantly worse (17–30%; corrected $p < 0.01$). In the simulation studies, when noise levels exceeded 10%, LORETA and LAURA had substantially smaller localisation errors than the other inverse solutions.
Conclusions: LORETA and LAURA provided the highest spatial accuracy both in clinical and simulated data, alongside with a comparably high robustness towards noise.
Significance: Among the different linear inverse solution algorithms tested, LORETA and LAURA might be preferred for interictal EEG source localisation.

1. Introduction

Electroencephalographic (EEG) source localisation (ESL) aims at identifying the sources of neural activity within the brain based on potential differences across scalp EEG electrodes. The most relevant clinical application of ESL is during presurgical diagnostic evaluation of patients with pharmacoresistant focal epilepsy. Among other localising tools, ESL is used to determine the sources of interictal epileptic EEG discharges and, less frequently, EEG seizure patterns (Mouthaan et al., 2016, Mouthaan et al., 2019, Zijlmans et al., 2019). The hereby identified brain areas serve as estimates for the theoretical epileptogenic zone which is 'indispensable for the generation of epileptic seizures' and needs to be

Abbreviations: CLARA, Classical LORETA recursively applied; cMEM, Coherent Maximum Entropy on the Mean; dSPM, Dynamic Statistical Parametric Mapping; EEG, Electroencephalograph; ESL, EEG Source Localisation; eLORETA, Exact Low-Resolution Electromagnetic Tomography; ILAE, International League Against Epilepsy; LAURA, Local Autoregressive Average; LORETA, Low-Resolution Electromagnetic Tomography; LSMAC, Locally Spherical Model with Anatomical Constraints; MEG, Magnetoencephalography; MN, Minimum Norm; sLORETA, Standardised Low-Resolution Electromagnetic Tomography; SMAC, Spherical Model with Anatomical Constraints; WMN, Weighted Minimum Norm.

* Corresponding author at: EEG and Epilepsy Unit, Epilepsy and Brain Networks Group, University Hospitals and Faculty of Medicine, University of Geneva, Rue Gabrielle-Perret-Gentil 4, 1205 Geneva, Switzerland.
E-mail addresses: bernd.vorderwuelbecke@charite.de, bernd.vorderwulbecke@etu.unige.ch (B.J. Vorderwülbecke).
[1] Permanent address: Epilepsy-Center Berlin-Brandenburg, Department of Neurology, Charité – Universitätsmedizin Berlin, Charitéplatz 1, 10117 Berlin, Germany.

https://doi.org/10.1016/j.clinph.2021.10.008
1388-2457/

eliminated for postsurgical seizure freedom (Rosenow and Lüders, 2001). In principle, ESL is based (1) on a biophysical head model or 'forward solution' to the forward problem, which EEG signal results from a given source activity inside the brain, and (2) an 'inverse solution' to the inverse problem, which pattern of source activity is the cause of a given EEG signal (Hauk et al., 2019). During the last five decades, a plethora of head models, inverse solutions, and software toolboxes have been proposed for ESL (Michel and Murray, 2012, He et al., 2018), with the accuracy of ESL results being highly dependent on the choice of the inverse solution (Mahjoory et al., 2017).

Distributed source models are based on thousands of dipolar sources with fixed orientations, regularly distributed within a 3-dimensional (3D) brain space or a cortical surface. The sources' activation is described as a current density distribution. As an advantage of distributed models, an *a priori* assumption on the number of active dipoles underlying a specific scalp voltage topography is not needed (Michel and Murray, 2012, He et al., 2018). Among the distributed source models, 'linear' models are based on the assumption that the potential recorded by any EEG electrode is a linear combination of the active brain sources' strengths, so that linear algebraic techniques can solve the inverse problem (Lagerlund, 1999).

Linear distributed inverse solutions are widely used for interictal ESL during presurgical evaluation of patients with pharmacoresistant focal epilepsy (Lascano et al., 2016, Centeno et al., 2017, Baroumand et al., 2018, Plummer et al., 2019). However, until now, a systematic comparison is missing as to which of these yields the most accurate interictal ESL results for presurgical epilepsy evaluation. With the study presented here, we aimed at assessing the accuracy of 6 different, clinically important linear distributed inverse solutions. As a brief overview, the Minimum Norm (MN) algorithm was proposed in 1994 to estimate source-current distributions as an alternative to single- or multi-dipole models (Hämäläinen and Ilmoniemi, 1994). As the MN tends to mislocalise deeper sources, the Weighted Minimum Norm (WMN) method compensates for this by means of a weighting matrix (Pascual-Marqui, 1999). The Low-Resolution Electromagnetic Tomography (LORETA) aims at finding the smoothest MN solution of EEG activity distribution (Pascual-Marqui et al., 1994), whereas the Local Autoregressive Average (LAURA) integrates biophysical assumptions in addition to purely mathematical constraints into the MN algorithm (Grave de Peralta Menendez et al., 2001). To allow for zero-error localisation, standardised LORETA (sLORETA) standardises the current density estimate given by the MN by using the covariance of the resolution matrix for post-hoc non-linear normalisation (Pascual-Marqui, 2002), while exact LORETA (eLORETA) uses iterative weighting to achieve exact localisation at least under noise-free conditions (Pascual-Marqui, 2007). For a more detailed overview see, for example, (Grech et al., 2008, (Pascual-Marqui et al., 2011), He et al., 2018, Samuelsson et al., 2020).

We took advantage of the fact that all 6 above-mentioned inverse solutions are implemented in one software toolbox, so that we could analyse them in parallel using the same processing and evaluation pipeline. The inverse solutions' spatial accuracy for high-density EEG source localisation was compared using averaged interictal discharges of patients with focal epilepsy. We used a clinical dataset in which we recently obtained optimal ESL results by spatial down-sampling of discharge averages from 257 to 204 EEG channels, at the time point of 50% of the discharge's rising phase (Vorderwülbecke et al., 2020). Consequently, we used 204 EEG channels and 50% of the rising phase also for the study presented here. The time point of 50% is a pragmatic and well-established compromise between a low probability of source propagation (towards the discharge's onset) and a high signal-to-noise ratio (towards its peak). In the literature, clinical validation of ESL accuracy is commonly based either on distance between the estimated source and the ultimately resected brain area or on (sub)lobar concordance of source estimate and resection (Mouthaan et al., 2019). To facilitate comparison with other studies, we assessed clinical accuracy in these both ways separately.

In addition, we aimed at replicating our clinical findings with the help of computer simulations and at investigating as to how the number of active sources and different levels of noise affect the precision of the different inverse solutions. To model the situation during an interictal epileptic discharge, we simulated a small number of active brain sources with different intensities and compared the inverse solution matrices' abilities to determine the source of maximum intensity. As there is always neuronal background activity in the brain (biological noise), we added different levels of spurious source activity as noise to the source space. Moreover, we added the same levels of noise to the sensor space to simulate the inevitable technical noise during EEG recording.

2. Methods

2.1. Patient cohort

Patient cohort and clinical methodology have recently been described in detail (Vorderwülbecke et al., 2020). For a schematic overview, see Fig. 1A. Briefly, the database of the EEG and Epilepsy Unit at the University Hospitals Geneva was retrospectively screened for patients with (1) a first resective brain surgery to treat pharmacoresistant focal epilepsy, (2) age > 6 years at evaluation, (3) presurgical 257-channel EEG recording with focal interictal epileptic discharges, (4) presurgical high-resolution MRI, and (5) known 12-month postsurgical outcome. Among 304 patients screened, 45 patients fulfilled the inclusion criteria (Vorderwülbecke et al., 2020). Thirty of these had no seizures for 12 months postoperatively, or auras only. This corresponds to the International League Against Epilepsy's (ILAE) surgical seizure outcome classes 1 or 2 (Wieser et al., 2001) and implies that the resected brain area contained the epileptogenic zone. Among these 30 patients, 19 had an anterior temporal lobe resection, 14 of these with amygdala-hippocampectomy, while the remaining 11 had extratemporal resections (Table 1; Supplementary Table 1). Temporal lobe resections affected 3 sublobes, while extratemporal resections affected 1–8 sublobes (median: 3; Supplementary Fig. 1). The study was approved by the local ethics committee of the province (canton) of Geneva. As clinical routine data were reused and individuals cannot be identified, the need for written informed consent was waived.

2.2. EEG recording and pre-processing

High-density EEG recordings (257 electrodes; unfiltered acquisition, sampling rate 500–1000 Hz) of 1–20 hours duration were acquired during presurgical epilepsy evaluation at the University Hospitals Geneva (Philips EGI, now Magstim EGI, Eugene, US-OR). Interictal epileptic discharges were identified visually and clustered based on topography and morphology. Discharges occurring earlier than 1 second after a previous discharge were not considered. If a patient had more than one discharge cluster, that one was selected which occurred most frequently while fitting to the clinical focus hypothesis. Five patients had more than one cluster, and in four of them, the most frequent discharge was chosen (patients no. 3, 7, 8, and 13; Supplementary Table 1). In the remaining patient, the number of single IEDs was unknown, and the cluster ipsilateral to the presumed focus was selected (patient no. 24). Alternative discharge clusters did not lead to better ESL results.

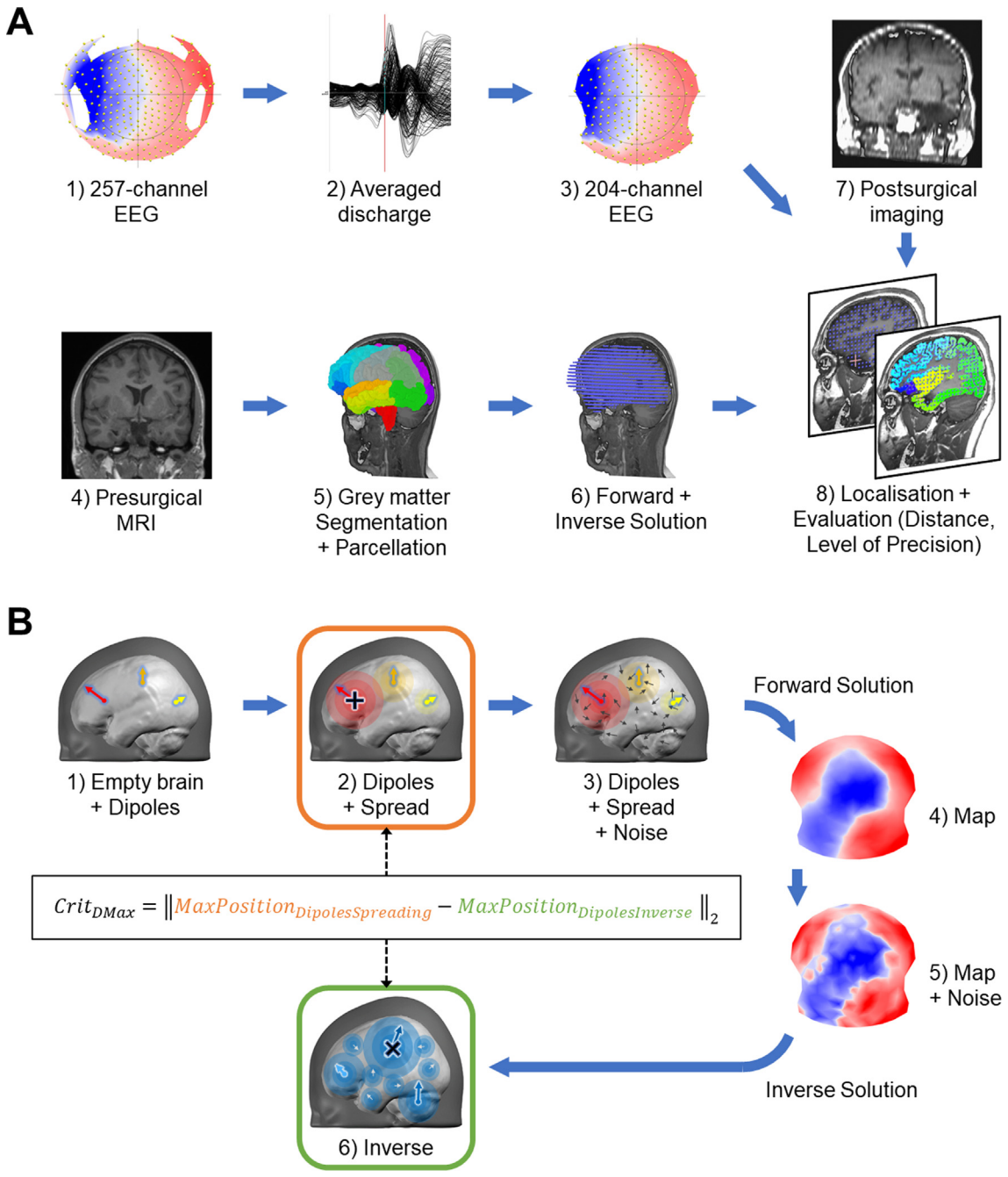

Fig. 1. Schematic illustration of the methodology. A, clinical data. From presurgical 257-channel EEG (1), interictal epileptic discharges were visually identified and averaged (2), followed by down-sampling to 204 channels (3). From individual high-resolution presurgical structural MRI (4), a grey matter mask was generated and parcelled into 38 sublobes (5). A 3-shell spherical model with anatomical constraints was built as forward model with 5000 solution points distributed within the grey matter, and one of the 6 different linear inverse solutions was applied (6). Postsurgical MRI or CT (7) was co-registered to the solution points grid. The source was localised as the solution point with maximum amplitude at 50% of the averaged discharge's rising phase. For evaluation, this localisation was compared to the edge of resection (distance) and to the affected (sub)lobes (level of precision; 8). – B, computer simulations. Localisation accuracy of the 6 inverse solutions was tested using 1 to 5 active dipolar sources with different intensities. Across n active sources, their intensities were set as linearly decreasing (n/n, (n-1)/n, . . ., 1/n) (1). The source spread was based on the inverse squared distance (2). Gaussian noise with increasing standard deviations of 0%, 10%, 20%, 30%, 40% and 50% of the input data was added, simultaneously in both source space (3) and EEG space (5). For each simulation, the localisation error (CritDMax) was assessed as the Euclidian distance between the source maximum given by the inverse solution (6, tilted cross) and the true source maximum (2, straight cross).

Epochs containing physiological artefacts surrounding the discharge were discarded following visual inspection. Already during presurgical evaluation, epochs were centred on the discharge's peak and averaged using the freely available Cartool software (Michel and Brunet, 2019). Raw EEG epochs and numbers of single discharges per average were not saved for later in 3 of the 30 patients (Supplementary Table 1). One-second averaged epochs were spatially down-sampled to 204 EEG channels by removal of cheek and neck electrodes using MATLAB R2016a (The MathWorks, Inc., Natick, US-MA) as detailed elsewhere (Vorderwülbecke et al., 2020). With Cartool 3.80 version 6164, epochs were filtered in the interval [1–70] Hz with a 4th-order Butterworth filter, plus notch

Table 1
Demographic and clinical data of the study cohort. Data are given as n (row %) or as median [interquartile range]. * n = 27 patients, since the number of single discharges is unknown in 3 patients.

Included patients		30
Sex	Female	21 (70%)
	Male	9 (30%)
Age at onset (years)		8 [1–14]
Age at surgery (years)		19 [12–30]
Hemisphere	Left	20 (67%)
	Right	10 (33%)
Localisation	Temporal	19 (63%)
	Extratemporal	11 (37%)
Structural MRI	Lesional	27 (90%)
	Non-lesional	3 (10%)
Number of single EEG discharges		23 [17–49] *

filtering at 50 Hz. Channels corrupted by technical artefacts were identified via visual inspection of EEG waveforms patterns and surface voltage maps and corrected via interpolation from nearby channels using 3D splines. Finally, averaged epochs were temporally down-sampled to 250 Hz.

2.3. MRI recording and head modelling

The head model was based on the patients' structural T1 or MPRAGE MRI re-sampled to 1 mm3 isotropic resolution using cubic interpolation. Based on anatomical landmarks, the 3D electrode grid was interactively co-registered to the individual head. In order to restrict the source space to the cerebral grey matter, a 3D grey matter mask was generated using FreeSurfer (version 6.0.1) (Reuter et al., 2012). With the use of the open-source Connectome Mapper 3 (Tourbier et al., 2019), this grey matter mask was parcelled into 38 sublobar areas (19 per hemisphere) not including brainstem and cerebellum (Daducci et al., 2012) to allow assessing (sub)lobar accuracy of ESL. Using Cartool, approximately 5,000 solution points were distributed equally in a 3D grid throughout the grey matter mask. A simplified realistic 3-shell head model, the Locally Spherical Model with Anatomical Constraints (LSMAC), with age-adjusted skull thickness served as head model for the 6 different linear distributed inverse solutions (Michel and Brunet, 2019). For interictal ESL, LSMAC was shown to perform similarly accurate to the more sophisticated head Boundary Element Model and Finite Element Model (Birot et al., 2014). The MN algorithm implemented in Cartool is L2-based (least squares).

2.4. Evaluation of clinical ESL accuracy

Averaged interictal epileptic discharges were subjected to ESL at 50% of their rising phase. Noise-dependent Tikhonov regularisation was applied. For a detailed description of the L-curve based regularisation procedure, see (Michel and Brunet, 2019). The default level of regularisation was 6–7 on a range from 0 to 12; if it was changed manually, localisation results remained stable. The patient's postsurgical MRI or computed tomography scan was resliced using SPM8 (Wellcome Centre for Human Neuroimaging, University College London, UK) and co-registered to the solution points' grid. Spatial accuracy of ESL was assessed semi-quantitatively in two ways: (1) the shortest distance between the source maximum and the border of the resection in one of the three orthogonal planes (0 mm = source maximum inside the resection, <10 mm, <20 mm, or > 20 mm); (2) the level of precision in relation to the 38 sublobar areas (source maximum within a sublobe or lobe affected by the resection, correct lateralisation, or contralateral hemisphere). Concordance of ESL was defined as the proportion of patients with (1) the source maximum being inside the resection (0 mm distance) or (2) sublobar concordance, respectively, in the 30 patients with favourable surgical outcome.

2.5. Simulated data

Analogously, based on 204 EEG electrodes, LSMAC, 5,018 solution points, and the Cartool software, localisation accuracy of the 6 inverse solutions was tested in computer simulations as a function of numbers of sources and levels of noise. The relative intensity of n (1 to 5) active sources was set as linearly decreasing (n/n, (n-1)/n, …, 1/n). For any given number of sources and for each inverse matrix, 20,072 random trials were performed. The sources' orientations were random, as well as their localisations, except for the first (maximum) source which was set to sequentially iterate through all solution points. Sources were not punctual but with intensity spreading to their neighbouring sources, with the spread being based on the inverse squared distance. Gaussian noise with increasing standard deviations of 0%, 10%, 20%, 30%, 40% and 50% of the input data was added to the signal simultaneously in both source space and EEG space (Fig. 1B). This allowed simulating different levels of background brain activity and electronic noise at the same time, while handling a single noise parameter. Noise-dependent Tikhonov regularisation at the default level (value = 3 on a range from 0 to 12) was applied (Michel and Brunet, 2019). The noise covariance was not included in the model; therefore, there was no hyperparameter tuning. For each simulation, the localisation error was assessed as the Euclidian distance between the source maximum given by the inverse solution and the real source maximum (*i.e.*, the centre of the source with intensity = 1, with all other sources acting as distractors).

2.6. Statistical analyses

All inverse solutions were compared to LAURA as the current default method for ESL in our epilepsy centre both for clinical and scientific purposes (Rubega et al., 2019, Carboni et al., 2020, Vorderwülbecke et al., 2020). Non-parametric data (distance to resection, level of precision) were subjected to two-sided Wilcoxon tests, and continuous data (localisation error) were subjected to two-sided dependent T tests. Within each set of 5 pairwise comparisons, p-values were corrected according to the Benjamini-Hochberg procedure, assuming a false discovery rate of 0.05 (Hemmerich, 2016). A corrected $p < 0.05$ was considered significant.

2.7. Data and code availability

Individual clinical results are detailed in Supplementary Fig. 1 and Supplementary Table 1. De-identified raw data of the whole 45-patient cohort will be made publicly available in a data repository (in preparation). The Cartool software is freely available for use in public research and non-commercial purposes (http://cartoolcommunity.unige.ch).

3. Results

3.1. Patient data

Using either LORETA or LAURA, the source maxima were located inside the resected brain areas in 57% or 50% ($p > 0.05$), whereas all other inverse solutions performed significantly worse (17–30%; $p < 0.01$ in comparison to LAURA; Fig. 2). In terms of sublobar concordance, results obtained with LAURA were correct in 83% while the other inverse solutions achieved 53–73%, but differences were

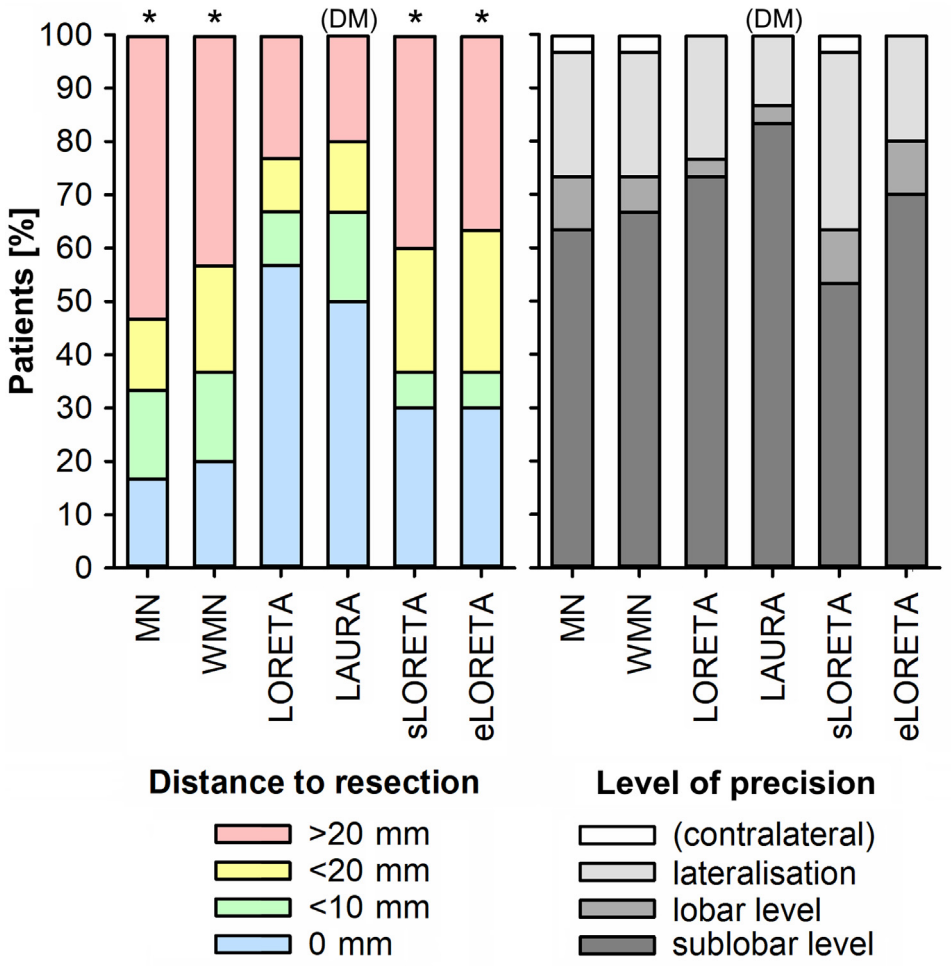

Fig. 2. Clinical spatial accuracies of ESL using the different inverse solutions. In 30 patients with focal epilepsy and favourable surgical outcome, ESL accuracies were measured as distances between maximum source and resected brain area (left, coloured bars) and levels of precision (right, greyscale bars). The source maximum being inside the resection (0 mm, blue) and sublobar concordance (darkest grey) were considered accurate. For individual results, see Supplementary Fig. 1. ESL, EEG source localisation; MN, Minimum Norm; WMN, Weighted Minimum Norm; LORETA, Low-Resolution Electromagnetic Tomography; LAURA, Local Autoregressive Average; sLORETA, standardised LORETA; eLORETA, exact LORETA; DM, default method. *, corrected $p < 0.01$ in pairwise comparison to LAURA, two-sided Wilcoxon test.

not statistically significant. Descriptively, individual results obtained with LORETA and LAURA were similar to each other, as were results obtained with MN and WMN, and, to a lesser extent, results obtained with sLORETA and eLORETA. If other inverse solutions than LORETA or LAURA were used, source maxima especially in temporal lobe epilepsy cases tended to shift towards ventrolateral prefrontal brain areas (Supplementary Fig. 1). If the predecessor of LSMAC, the Spherical Model with Anatomical Constraints (SMAC) (Spinelli et al., 2000), served as the head model for LAURA, spatial accuracy was lower than with LSMAC (Supplementary Fig. 2 AC). Generally, ESL results tended to be more accurate with higher numbers of averaged single discharges (Supplementary Table 1).

3.2. Simulated data

For each inverse solution tested, results were most accurate in case of a single active source and no noise. In this specific constellation, eLORETA and sLORETA always localised the active source with zero error, while LORETA and LAURA both had average localisation errors of about 16 mm, and MN and WMN of > 23 mm (Fig. 3 AB). Errors in localising the maximum source increased with both increasing numbers of active sources and increasing levels of noise. In case of zero noise, sLORETA and eLORETA remained the most accurate solutions for all number of sources tested. However, with noise levels above 10%, LORETA and LAURA had the smallest localisation errors across all inverse solutions tested, irrespective of the number of active sources (Fig. 3). When simulated results from all tested numbers of sources (1–5) and all levels of noise (0–50%) were merged, median localisation errors were 27 mm (interquartile range, 11–81) for LORETA and 32 mm (11–83) for LAURA but above 50 mm for all other inverse solutions (Fig. 4).

4. Discussion

We evaluated the spatial accuracy of 6 different linear distributed inverse solutions by localising both 'real-data' sources of human interictal epileptic activity and computer-simulated brain sources. Both types of analysis congruently and independently show that among the algorithms tested, LORETA and LAURA provide the highest spatial accuracies. In addition, our computer simulations demonstrate that the inverse solutions' performance highly depends on both the number of active sources within the brain and the level of noise added to the signal.

4.1. Added value of this study

More than the choice of the forward model, the selection of a specific inverse solution, subspace constraint and/or software toolbox has been shown to substantially influence the accuracy of ESL both of physiological brain activity (Mahjoory et al., 2017) and

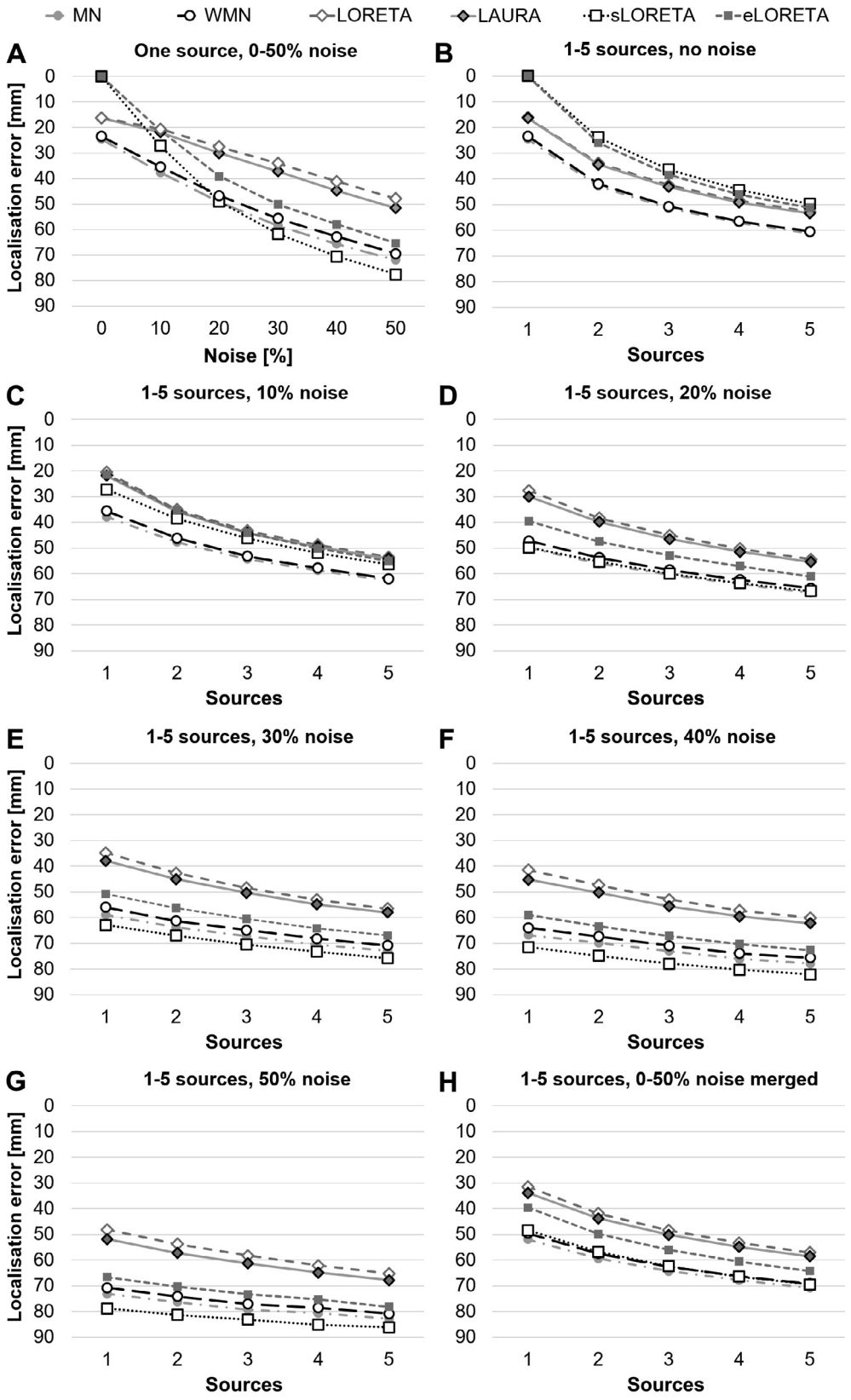

Fig. 3. Simulated spatial accuracies of ESL depending on the number of sources and the level of noise. Localisation errors were measured as Euclidian distances between estimated and true source maxima. Symbols indicate the means of 20,072 simulations (A-G) or 120,432 simulations (H). ESL, EEG source localisation; MN, Minimum Norm; WMN, Weighted Minimum Norm; LORETA, Low-Resolution Electromagnetic Tomography; LAURA, Local Autoregressive Average; sLORETA, standardised LORETA; eLORETA, exact LORETA. **, corrected $p < 0.0001$ in pairwise comparison to LAURA, two-sided T test.

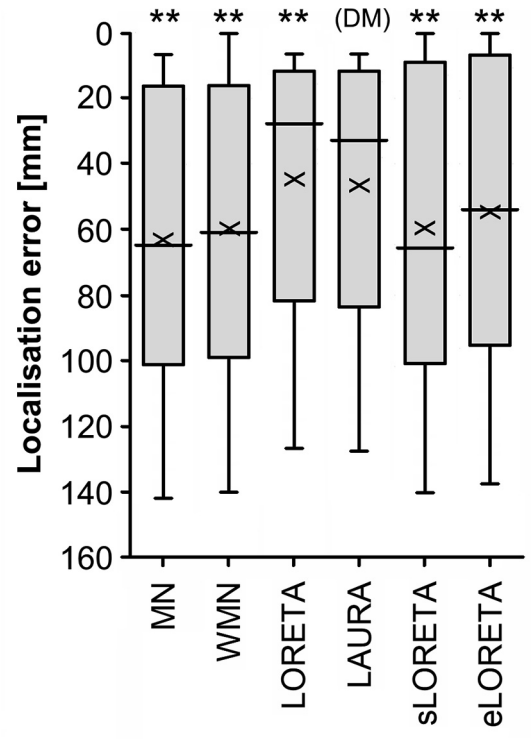

Fig. 4. Simulated spatial accuracies of ESL across all numbers of sources and levels of noise tested. ESL accuracies were measured as localisation errors between estimated and true source maxima. Per inverse solution, 602,160 simulations were run with different numbers of sources (1–5) and different levels of noise (0–50%). The box-whisker plots give the 2.5th, 25th, 50th, 75th, and 97.5th percentile, with the X indicating the mean. ESL, EEG source localisation; MN, Minimum Norm; WMN, Weighted Minimum Norm; LORETA, Low-Resolution Electromagnetic Tomography; LAURA, Local Autoregressive Average; sLORETA, standardised LORETA; eLORETA, exact LORETA; DM, default method. **, corrected $p < 0.0001$ in comparison to LAURA, two-sided T test.

interictal epileptic discharges (Plummer et al., 2010b). Distributed source models have been shown to be similarly accurate as single dipole models for ictal and interictal ESL (Waberski et al., 2000, Plummer et al., 2010a, Beniczky et al., 2016, Strobbe et al., 2016, Sharma et al., 2018, Duez et al., 2019, Ricci et al., 2021). However, the performance of different distributed inverse solutions has not yet been systematically compared for interictal ESL in patients with epilepsy. Besides one study comparing one non-linear to two linear distributed inverse models (Heers et al., 2016) (see below), the work presented here is the first to systematically evaluate different representatives of one class of inverse solutions for interictal ESL based on both clinical and simulated data. Both types of analysis consistently indicate that LORETA and LAURA are similarly well suited for EEG source localisation of interictal epileptic discharges. Interestingly, both outperform not only the classical MN and WMN algorithms, but also the newer sLORETA and eLORETA. This is of special importance because sLORETA is among the trending inverse solutions for interictal and ictal ESL in presurgical epilepsy evaluation (Baroumand et al., 2018, Duez et al., 2019, Habib et al., 2020, Vespa et al., 2020, Ricci et al., 2021, Ye et al., 2021).

4.2. Validity of clinical data

Our clinical data stem from 30 patients who became seizure-free after brain surgery. Therefore, concordance of source maximum and the area of resection is highly indicative of correct source localisation. To increase accuracy, we based our analysis on individual high-resolution MRI. Caudal channels were removed from the original 257-channel EEG because we recently found that this both decreased the workload and increased the accuracy of the results at least when using the LSMAC head model (Vorderwülbecke et al., 2020).

Following two recent meta-analyses, interictal ESL is reported to colocalise with the resected brain area in 81–87% of patients with successful epilepsy surgery (Mouthaan et al., 2019, Sharma et al., 2019). The concordance rates of 50–83% in our specific patient group are somewhat lower but basically within a similar range (Vorderwülbecke et al., 2020). Accuracy was higher in temporal lobe epilepsy than in extratemporal epilepsy (Supplementary Figs. 1-2 and Supplementary Table 1) which is consistent with several other studies (Brodbeck et al., 2011, Coutin-Churchman et al., 2012, van Mierlo et al., 2017) but not all (Abdallah et al., 2017). For a detailed discussion of this phenomenon, see Vorderwülbecke et al. (2020).

4.3. Effects of source numbers and noise levels

As already shown by Grave de Peralta Menendez et al. (2001), we corroborate that both LORETA and LAURA achieve substantially smaller localisation errors than MN and WMN in noise-free simulated data. We also confirm that the two most recently developed algorithms, sLORETA and eLORETA, can perfectly localise single sources under noise-free conditions (Pascual-Marqui, 2007, Pascual-Marqui et al., 2011). However, consistent with the literature (Samuelsson et al., 2020), localisation accuracy of all tested inverse solutions degraded as soon as there were more than one active source and/or noise of at least 10%, which is more representative of clinical data. From a physiological perspective, single source scenarios are hardly to be expected in the brain. The actual benefit of distributed inverse solutions is that several dipoles can be localised without the need to define their number in the model *a priori*.

With regard to noise, our simulated data show that LORETA and LAURA are comparably robust towards it, whereas the excellent performance of sLORETA and especially eLORETA under noise-free conditions substantially worsens with increasing noise levels. This is reflected by an only intermediate performance of sLORETA and eLORETA if applied on the clinical data. Therefore, even if epileptic discharges are averaged to increase the signal-to-noise ratio, background and recording noise cannot be neglected.

4.4. Other comparative studies

In contrast to our findings, a smaller clinical study on 8 patients with temporal lobe epilepsy reported advantages of sLORETA over LORETA: Plummer et al. (2010b) found that sLORETA led to more consistent interictal low-density ESL results than LORETA, MN least squares, or Minimum L1 Norm. In our study now, LORETA and LAURA were superior to sLORETA in both temporal and extratemporal epilepsy (Supplementary Fig. 2). This discrepancy is most likely due to methodological differences. Plummer et al. used a 'best-fit' approach based on the highest achievable current density of any dipole at any time of the spike's rising phase, following independent component analysis of the original signal. Instead, we always used the discharge's half-rise and no signal separation procedures.

Heers et al. (2016) compared their Coherent Maximum Entropy on the Mean algorithm (cMEM, a non-linear probabilistic Bayesian approach) to the Independent and Identically Distributed model (which is similar to the MN) and the Spatially Coherent Sources model (comparable to LORETA). They used interictal discharges of 15 patients with focal epilepsy, recorded with simultaneous scalp EEG and MEG, as well as computer-simulated discharges.

Concordance with intracranial EEG results was similar across the three models if applied on the scalp EEG discharges, but cMEM outperformed the other two models if applied on the MEG discharges. In addition, cMEM most accurately recovered the spatial extent of simulated sources. In a follow-up study on interictal MEG source localisation in 28 patients with mostly extratemporal epilepsy, Pellegrino et al. (2020) found that sLORETA yielded minimally smaller localisation errors than the cMEM, the MN, and the Dynamic Statistical Parametric Mapping (dSPM, a noise-normalised descendent of MN) algorithms. Our data now indicate that for EEG discharges, LORETA outperforms sLORETA thanks to a lower susceptibility to noise. A formal comparison to cMEM was beyond the scope of our study but should be addressed in the future.

Interestingly, Pellegrino et al. (2020) achieved the best performance using an average of the source intensity maps given by their four algorithms. Like others before them, *e.g.*, (Grova et al. (2006), Plummer et al. (2010a), the authors proposed to combine information from different inverse solutions. Since our validation approach was based on visual evaluation of given source activation maps, at it is done in clinical practice, we were not able to integrate the results of different algorithms. However, meaningful combinations of different ESL methods seem to be a promising avenue for the future.

4.5. Limitations and outlook

For the study presented here, we deliberately focused on one specific software package. This comes both as a strength and a limitation of our approach. On the one hand, we avoided the influence of inter-software variability on our results (Mahjoory et al., 2017). On the other hand, we were not able to evaluate further linear distributed inverse models like dSPM (Dale et al., 2000) or Classical LORETA Analysis Recursively Applied (CLARA) (Beniczky et al., 2016) because they are not implemented in the Cartool software. In fact, Cartool does contain a seventh inverse solution named 'sDale' that is based on a predecessor of dSPM (Dale and Sereno, 1993). This yielded intermediate results (Supplementary Fig. 2 AB) which we did not include in the main analysis because, to our knowledge, 'sDale' does not play a relevant role in presurgical epilepsy evaluations. As another limitation, due to the averaging of short spike epochs, we were not able to assess the signal-to-noise ratios of our clinical data in a manner that would have been comparable to the simulated data. Nevertheless, the computer simulations clearly indicate that the comparably strong performance of LORETA and LAURA is explained by their higher robustness towards noise.

Our approach was based on a typical clinical workflow. Interictal epileptic discharges were selected and averaged already during the patients' presurgical evaluation, based on expert opinion rather than on prespecified objective criteria (Abdallah et al., 2017). Electrodes were co-registered to the MRI manually. The resulting imprecision and the effect of the sources' depth cannot be quantified in our study. For simplicity, we focused on the source maximum to define its localisation error. However, distributed source imaging specifically allows assessing the extent of source activation (Plummer et al., 2010b). As another measure of ESL accuracy, spatial dispersion accounts for both localisation error and the reconstructed sources' spread (Chowdhury et al., 2016, Pellegrino et al., 2020, Samuelsson et al., 2020). Additional thresholding methods allow assessing further spatial characteristics of source activation (Pellegrino et al., 2020). These should be considered in future comparative studies.

We used averaged discharges, but alternatively, single discharges can be localised to statistically evaluate the distribution of their respective sources (Plummer et al., 2010a, Rikir et al., 2014). Our source space consisted of a regular 3D grid throughout the grey matter while other approaches are based on a single layer of sources at the cortical surface (Pellegrino et al., 2020, Samuelsson et al., 2020). Both should be compared to each other in the future. Finally, it would be of high interest to contrast our ESL results with those achieved with equivalent current dipole fitting (Plummer et al., 2010a, Beniczky et al., 2016). This is not straightforward because dipole fitting gives a 'centre of mass' rather than a point of maximum activation, and parts of the information are contained in the dipole's orientation, not only in its position. All these endeavours would have been beyond the scope of the study presented here but should be addressed as a next step.

Direct comparisons of ESL results across studies are difficult because of diverging validation approaches and cohorts. Therefore, to enable other research groups in the field to directly compare their methodological pipelines to ours, we plan to make the de-identified patient data of our cohort (MRI, averaged discharges) freely available to the community, together with a detailed data descriptor paper (in preparation). This will allow validation of various head models, inverse solution algorithms, and software packages for interictal ESL in a large group of patients with pharmacoresistant focal epilepsy, 257-channel EEG, and known 12-month postsurgical seizure outcome as a ground truth. The overall aim is to better evaluate accuracy and clinical added value of ESL to assist in localising the epileptogenic zone and, therefore, to help tailoring implantation of intracranial electrodes and/or surgical resections.

5. Conclusions

Our study strengthens the view that the choice of an inverse model for ESL should be made with great care, depending on the type of signal and the level of noise. Based on the results shown above, sLORETA or eLORETA may be considered for data with less than 10% noise (*i.e.*, signal-to-noise ratios of > 10). For ESL of interictal epileptic discharges, more noise-robust inverse solutions as LORETA and LAURA promise more accurate ESL results. For the future, further systematic studies are needed to compare other inverse solutions within and beyond their classes, and finally across software toolboxes.

CRediT authorship contribution statement

Margherita Carboni: Conceptualization, Data curation, Investigation, Validation, Writing – review & editing. **Denis Brunet:** Software, Investigation, Formal analysis, Validation, Visualization, Writing – original draft, Writing – review & editing. **Martin Seeber:** Validation, Writing – original draft, Writing – review & editing. **Christoph M. Michel:** Resources, Supervision, Writing – review & editing. **Serge Vulliemoz:** Funding acquisition, Resources, Supervision, Writing – review & editing. **Bernd J. Vorderwülbecke:** Conceptualization, Investigation, Formal analysis, Visualization, Writing – original draft, Writing – review & editing.

Declaration of Competing Interest

S. Vulliemoz is shareholder and advisor of Epilog NV (Ghent, BE). All other authors declare that they have no known competing financial interests or personal relationships that could have appeared to influence the work reported in this paper.

Acknowledgements

This study was funded by the Swiss National Science Foundation [grants SNSF 169198, 192749, and CRSII5 170873 to S. Vul-

liemoz] and the German Research Foundation [grant DFG 422589384 to B. J. Vorderwülbecke]. The funders were not involved in the study design, in the collection, analysis and interpretation of data, in the writing of the report, or in the decision to submit the article for publication. – The Cartool software (cartoolcommunity.unige.ch) has been programmed by D. Brunet from the Functional Brain Mapping Laboratory (FBMLab), Geneva, Switzerland, and is supported by the Center for Biomedical Imaging (CIBM) of Geneva and Lausanne, Switzerland. – The authors wish to thank M. Seeck MD, L. Spinelli PhD, S. Tourbier PhD, and J. Wirsich PhD for their valuable support.

Appendix A. Supplementary material

Supplementary data to this article can be found online at https://doi.org/10.1016/j.clinph.2021.10.008.

References

Abdallah C, Maillard LG, Rikir E, Jonas J, Thiriaux A, Gavaret M, Bartolomei F, Colnat-Coulbois S, Vignal J-P, Koessler L. Localizing value of electrical source imaging: Frontal lobe, malformations of cortical development and negative MRI related epilepsies are the best candidates. Neuroimage Clin 2017;16:319–29. https://doi.org/10.1016/j.nicl.2017.08.009.

Baroumand AG, van Mierlo P, Strobbe G, Pinborg LH, Fabricius M, Rubboli G, Leffers A-M, Uldall P, Jespersen Bo, Brennum J, Henriksen OM, Beniczky S. Automated EEG source imaging: a retrospective, blinded clinical validation study. Clin Neurophysiol 2018;129(11):2403–10. https://doi.org/10.1016/j.clinph.2018.09.015.

Beniczky S, Rosenzweig I, Scherg M, Jordanov T, Lanfer B, Lantz G, Larsson PG. Ictal EEG source imaging in presurgical evaluation: High agreement between analysis methods. Seizure 2016;43:1–5. https://doi.org/10.1016/j.seizure.2016.09.017.

Birot G, Spinelli L, Vulliémoz S, Mégevand P, Brunet D, Seeck M, Michel CM. Head model and electrical source imaging: a study of 38 epileptic patients. Neuroimage Clin 2014;5:77–83. https://doi.org/10.1016/j.nicl.2014.06.005.

Brodbeck V, Spinelli L, Lascano AM, Wissmeier M, Vargas M-I, Vulliemoz S, Pollo C, Schaller K, Michel CM, Seeck M. Electroencephalographic source imaging: a prospective study of 152 operated epileptic patients. Brain 2011;134(10):2887–97. https://doi.org/10.1093/brain/awr243.

Carboni M, De Stefano P, Vorderwülbecke BJ, Tourbier S, Mullier E, Rubega M, Momjian S, Schaller K, Hagmann P, Seeck M, Michel CM, van Mierlo P, Vulliemoz S. Abnormal directed connectivity of resting state networks in focal epilepsy. Neuroimage Clin 2020;27:102336. https://doi.org/10.1016/j.nicl.2020.102336.

Centeno M, Tierney TM, Perani S, Shamshiri EA, St Pier K, Wilkinson C, Konn D, Vulliemoz S, Grouiller F, Lemieux L, Pressler RM, Clark CA, Cross JH, Carmichael DW. Combined electroencephalography-functional magnetic resonance imaging and electrical source imaging improves localization of pediatric focal epilepsy. Ann Neurol 2017;82(2):278–87. https://doi.org/10.1002/ana.v82.210.1002/ana.25003.

Chowdhury RA, Merlet I, Birot G, Kobayashi E, Nica A, Biraben A, Wendling F, Lina JM, Albera L, Grova C. Complex patterns of spatially extended generators of epileptic activity: Comparison of source localization methods cMEM and 4-ExSo-MUSIC on high resolution EEG and MEG data. Neuroimage 2016;143:175–95. https://doi.org/10.1016/j.neuroimage.2016.08.044.

Coutin-Churchman PE, Wu JY, Chen LL, Shattuck K, Dewar S, Nuwer MR. Quantification and localization of EEG interictal spike activity in patients with surgically removed epileptogenic foci. Clin Neurophysiol 2012;123(3):471–85. https://doi.org/10.1016/j.clinph.2011.08.007.

Daducci A, Gerhard S, Griffa A, Lemkaddem A, Cammoun L, Gigandet X, et al. The connectome mapper: an open-source processing pipeline to map connectomes with MRI. PLoS One 2012;7(12). https://doi.org/10.1371/journal.pone.0048121.

Dale AM, Liu AK, Fischl BR, Buckner RL, Belliveau JW, Lewine JD, Halgren E. Dynamic statistical parametric mapping: combining fMRI and MEG for high-resolution imaging of cortical activity. Neuron 2000;26(1):55–67. https://doi.org/10.1016/S0896-6273(00)81138-1.

Dale AM, Sereno MI. Improved Localizadon of Cortical Activity by Combining EEG and MEG with MRI Cortical Surface Reconstruction: A Linear Approach. J Cogn Neurosci 1993;5(2):162–76. https://doi.org/10.1162/jocn.1993.5.2.162.

Duez L, Tankisi H, Hansen PO, Sidenius P, Sabers A, Pinborg LH, Fabricius M, Rásonyi G, Rubboli G, Pedersen B, Leffers A-M, Uldall P, Jespersen Bo, Brennum J, Henriksen OM, Fuglsang-Frederiksen A, Beniczky S. Electromagnetic source imaging in presurgical workup of patients with epilepsy: A prospective study. Neurology 2019;92(6):e576–86. https://doi.org/10.1212/WNL.0000000000006877.

Grave de Peralta Menendez R, Gonzalez Andino SL, Lantz G, Michel CM, Landis T. Noninvasive localization of electromagnetic epileptic activity. I. Method descriptions and simulations. Brain Topogr 2001;14(2):131–7.

Grech R, Cassar T, Muscat J, Camilleri KP, Fabri SG, Zervakis M, Xanthopoulos P, Sakkalis V, Vanrumste B. Review on solving the inverse problem in EEG source analysis. J Neuroeng Rehabil 2008;5(1). https://doi.org/10.1186/1743-0003-5-25.

Grova C, Daunizeau J, Lina JM, Benar CG, Benali H, Gotman J. Evaluation of EEG localization methods using realistic simulations of interictal spikes. Neuroimage 2006;29(3):734–53. https://doi.org/10.1016/j.neuroimage.2005.08.053.

Habib MA, Ibrahim F, Mohktar MS, Kamaruzzaman SB, Lim KS. Recursive independent component analysis (ICA)-decomposition of ictal EEG to select the best ictal component for EEG source imaging. Clin Neurophysiol 2020;131(3):642–54. https://doi.org/10.1016/j.clinph.2019.11.058.

Hämäläinen MS, Ilmoniemi RJ. Interpreting magnetic fields of the brain: minimum norm estimates. Med Biol Eng Comput 1994;32(1):35–42. https://doi.org/10.1007/BF02512476.

Hauk O, Stenroos M, Treder M. EEG/MEG Source Estimation and Spatial Filtering: The Linear Toolkit. Cham: Magnetoencephalography. Springer; 2019.

He B, Sohrabpour A, Brown E, Liu Z. Electrophysiological Source Imaging: A Noninvasive Window to Brain Dynamics. Annu Rev Biomed Eng 2018;20(1):171–96. https://doi.org/10.1146/annurev-bioeng-062117-120853.

Heers M, Chowdhury RA, Hedrich T, Dubeau F, Hall JA, Lina J-M, Grova C, Kobayashi E. Localization Accuracy of Distributed Inverse Solutions for Electric and Magnetic Source Imaging of Interictal Epileptic Discharges in Patients with Focal Epilepsy. Brain Topogr 2016;29(1):162–81. https://doi.org/10.1007/s10548-014-0423-1.

Hemmerich W. Rechner zur Adjustierung des α-Niveaus: StatistikGuru, https://statistikguru.de/rechner/adjustierung-des-alphaniveaus.html; 2016 [Accessed 21.07.2020].

Lagerlund TD. EEG source localization (Model-dependent and model-independent methods). In: Niedermeyer E, Lopes da Silva F, editors. Electroencephalography: Basic principles, clinical applications, and related fields. Baltimore, US-MD: Williams & Wilkins; 1999, p. 809-22.

Lascano AM, Perneger T, Vulliemoz S, Spinelli L, Garibotto V, Korff CM, et al. Yield of MRI, high-density electric source imaging (HD-ESI), SPECT and PET in epilepsy surgery candidates. Clin Neurophysiol 2016;127(1):150-5. S1388-2457(15)00314-4 [pii];10.1016/j.clinph.2015.03.025 [doi]

Mahjoory K, Nikulin VV, Botrel L, Linkenkaer-Hansen K, Fato MM, Haufe S. Consistency of EEG source localization and connectivity estimates. Neuroimage 2017;152:590–601. https://doi.org/10.1016/j.neuroimage.2017.02.076.

Michel CM, Brunet D. EEG Source Imaging: A Practical Review of the Analysis Steps. Front Neurol 2019;10:325. https://doi.org/10.3389/fneur.2019.00325 [doi].

Michel CM, Murray MM. Towards the utilization of EEG as a brain imaging tool. Neuroimage 2012;61(2):371-85. S1053-8119(11)01441-8 [pii];10.1016/j.neuroimage.2011.12.039 [doi]

Mouthaan BE, Rados M, Barsi P, Boon P, Carmichael DW, Carrette E, Craiu D, Cross JH, Diehl B, Dimova P, Fabo D, Francione S, Gaskin V, Gil-Nagel A, Grigoreva E, Guekht A, Hirsch E, Hecimovic H, Helmstaedter C, Jung J, Kalviainen R, Kelemen A, Kimiskidis V, Kobulashvili T, Krsek P, Kuchukhidze G, Larsson PG, Leitinger M, Lossius MI, Luzin R, Malmgren K, Mameniskiene R, Marusic P, Metin B, Özkara C, Pecina H, Quesada CM, Rugg-Gunn F, Rydenhag B, Ryvlin P, Scholly J, Seeck M, Staack AM, Steinhoff BJ, Stepanov V, Tarta-Arsene O, Trinka E, Uzan M, Vogt VL, Vos SB, Vulliémoz S, Huiskamp G, Leijten FSS, Van Eijsden P, Braun KPJ. Current use of imaging and electromagnetic source localization procedures in epilepsy surgery centers across Europe. Epilepsia 2016;57(5):770–6. https://doi.org/10.1111/epi.2016.57.issue-510.1111/epi.13347.

Mouthaan BE, Rados M, Boon P, Carrette E, Diehl B, Jung J, Kimiskidis V, Kobulashvili T, Kuchukhidze G, Larsson PG, Leitinger M, Ryvlin P, Rugg-Gunn F, Seeck M, Vulliémoz S, Huiskamp G, Leijten FSS, Van Eijsden P, Trinka E, Braun KPJ. Diagnostic accuracy of interictal source imaging in presurgical epilepsy evaluation: A systematic review from the E-PILEPSY consortium. Clin Neurophysiol 2019;130(5):845–55. https://doi.org/10.1016/j.clinph.2018.12.016.

Pascual-Marqui RD. Review of methods for solving the EEG inverse problem. Int J Bioelectromagn 1999;1(1):75–86.

Pascual-Marqui RD. Standardized low-resolution brain electromagnetic tomography (sLORETA): technical details. Methods Find Exp Clin Pharmacol 2002;24 Suppl D:5–12..

Pascual-Marqui RD. 3D distributed, linear imaging methods of electric neuronal activity. Part 1: Exact, zero error localization. Math Physics Biol Physics Neurons Cogn 2007;0710.

Pascual-Marqui RD, Lehmann D, Koukkou M, Kochi K, Anderer P, Saletu B, et al. Assessing interactions in the brain with exact low-resolution electromagnetic tomography. Philos Trans A Math Phys Eng Sci 2011 1952;369:3768–84. https://doi.org/10.1098/rsta.2011.0081.

Pascual-Marqui RD, Michel CM, Lehmann D. Low resolution electromagnetic tomography: a new method for localizing electrical activity in the brain. Int J Psychophysiol 1994;18(1):49–65.

Pellegrino G, Hedrich T, Porras-Bettancourt M, Lina J-M, Aydin Ü, Hall J, Grova C, Kobayashi E. Accuracy and spatial properties of distributed magnetic source imaging techniques in the investigation of focal epilepsy patients. Hum Brain Mapp 2020;41(11):3019–33. https://doi.org/10.1002/hbm.v41.1110.1002/hbm.24994.

Plummer C, Vogrin SJ, Woods WP, Murphy MA, Cook MJ, Liley DTJ. Interictal and ictal source localization for epilepsy surgery using high-density EEG with MEG:

a prospective long-term study. Brain 2019;142(4):932–51. https://doi.org/10.1093/brain/awz015.
Plummer C, Wagner M, Fuchs M, Harvey AS, Cook MJ. Dipole versus distributed EEG source localization for single versus averaged spikes in focal epilepsy. J Clin Neurophysiol 2010a;27(3):141–62. https://doi.org/10.1097/WNP.0b013e3181dd5004.
Plummer C, Wagner M, Fuchs M, Vogrin S, Litewka L, Farish S, Bailey C, Harvey AS, Cook MJ. Clinical utility of distributed source modelling of interictal scalp EEG in focal epilepsy. Clin Neurophysiol 2010b;121(10):1726–39. https://doi.org/10.1016/j.clinph.2010.04.002.
Reuter M, Schmansky NJ, Rosas HD, Fischl B. Within-subject template estimation for unbiased longitudinal image analysis. Neuroimage 2012;61(4):1402–18. https://doi.org/10.1016/j.neuroimage.2012.02.084.
Ricci L, Tamilia E, Alhilani M, Alter A, Scott Perry , Madsen JR, Peters JM, Pearl PL, Papadelis C. Source imaging of seizure onset predicts surgical outcome in pediatric epilepsy. Clin Neurophysiol 2021;132(7):1622–35. https://doi.org/10.1016/j.clinph.2021.03.043.
Rikir E, Koessler L, Gavaret M, Bartolomei F, Colnat-Coulbois S, Vignal J-P, Vespignani H, Ramantani G, Maillard LG. Electrical source imaging in cortical malformation-related epilepsy: a prospective EEG-SEEG concordance study. Epilepsia 2014;55(6):918–32. https://doi.org/10.1111/epi.2014.55.issue-610.1111/epi.12591.
Rosenow F, Lüders H. Presurgical evaluation of epilepsy. Brain 2001;124:1683–700.
Rubega M, Carboni M, Seeber M, Pascucci D, Tourbier S, Toscano G, Van Mierlo P, Hagmann P, Plomp G, Vulliemoz S, Michel CM. Estimating EEG Source Dipole Orientation Based on Singular-value Decomposition for Connectivity Analysis. Brain Topogr 2019;32(4):704–19. https://doi.org/10.1007/s10548-018-0691-2.
Samuelsson JG, Peled N, Mamashli F, Ahveninen J, Hämäläinen MS. Spatial fidelity of MEG/EEG source estimates: A general evaluation approach. Neuroimage 2021;224:117430. https://doi.org/10.1016/j.neuroimage.2020.117430.
Sharma P, Scherg M, Pinborg LH, Fabricius M, Rubboli G, Pedersen B, Leffers A-M, Uldall P, Jespersen B, Brennum J, Henriksen OM, Beniczky S. Ictal and interictal electric source imaging in pre-surgical evaluation: a prospective study. Eur J Neurol 2018;25(9):1154–60. https://doi.org/10.1111/ene.2018.25.issue-910.1111/ene.13676.
Sharma P, Seeck M, Beniczky S. Accuracy of Interictal and Ictal Electric and Magnetic Source Imaging: A Systematic Review and Meta-Analysis. Front Neurol 2019;10:1250. https://doi.org/10.3389/fneur.2019.01250.
Spinelli L, Andino SG, Lantz G, Seeck M, Michel CM. Electromagnetic inverse solutions in anatomically constrained spherical head models. Brain Topogr 2000;13(2):115–25.
Strobbe G, Carrette E, López JD, Montes Restrepo V, Van Roost D, Meurs A, Vonck K, Boon P, Vandenberghe S, van Mierlo P. Electrical source imaging of interictal spikes using multiple sparse volumetric priors for presurgical epileptogenic focus localization. Neuroimage Clin 2016;11:252–63. https://doi.org/10.1016/j.nicl.2016.01.017.
Tourbier S, Aleman-Gomez Y, Griffa A, Hagmann P. connectomicslab/connectomemapper3: Connectome Mapper v3.0.0-beta-20190815. Zenodo 2019.
van Mierlo P, Strobbe G, Keereman V, Birot G, Gadeyne S, Gschwind M, Carrette E, Meurs A, Van Roost D, Vonck K, Seeck M, Vulliémoz S, Boon P. Automated long-term EEG analysis to localize the epileptogenic zone. Epilepsia Open 2017;2(3):322–33. https://doi.org/10.1002/epi4.12066.
Vespa S, Baroumand AG, Ferrao Santos S, Vrielynck P, de Tourtchaninoff M, Feys O, Strobbe G, Raftopoulos C, van Mierlo P, El Tahry R. Ictal EEG source imaging and connectivity to localize the seizure onset zone in extratemporal lobe epilepsy. Seizure 2020;78:18–30. https://doi.org/10.1016/j.seizure.2020.03.001.
Vorderwülbecke BJ, Carboni M, Tourbier S, Brunet D, Seeber M, Spinelli L, Seeck M, Vulliemoz S. High-density Electric Source Imaging of interictal epileptic discharges: How many electrodes and which time point? Clin Neurophysiol 2020;131(12):2795–803. https://doi.org/10.1016/j.clinph.2020.09.018.
Waberski TD, Gobbele R, Herrendorf G, Steinhoff BJ, Kolle R, Fuchs M, et al. Source reconstruction of mesial-temporal epileptiform activity: comparison of inverse techniques. Epilepsia 2000;41(12):1574–83. https://doi.org/10.1111/j.1499-1654.2000.001574.x.
Wieser HG, Blume WT, Fish D, Goldensohn E, Hufnagel A, King D, et al. ILAE Commission Report. Proposal for a new classification of outcome with respect to epileptic seizures following epilepsy surgery. Epilepsia 2001;42(2):282–6.
Ye S, Yang L, Lu Y, Kucewicz MT, Brinkmann B, Nelson C, Sohrabpour A, Worrell GA, He B. Contribution of Ictal Source Imaging for Localizing Seizure Onset Zone in Patients With Focal Epilepsy. Neurology 2021;96(3):e366–75. https://doi.org/10.1212/WNL.0000000000011109.
Zijlmans M, Zweiphenning W, van Klink N. Changing concepts in presurgical assessment for epilepsy surgery. Nat Rev Neurol 2019;15(10):594–606. https://doi.org/10.1038/s41582-019-0224-y.